


## Article

# Vineyard Pruning Weight Prediction Using 3D Point Clouds Generated from UAV Imagery and Structure from Motion Photogrammetry

Marta García-Fernández , Enoc Sanz-Ablanedo , Dimas Pereira-Obaya  and José Ramón Rodríguez-Pérez 

Grupo de Investigación en Geomática e Ingeniería Cartográfica (GEOINCA), Universidad de León, Avenida de Astorga sn, 24401 Ponferrada, Spain; esana@unileon.es (E.S.-A.); dperep01@estudiantes.unileon.es (D.P.-O.); jr.rodriguez@unileon.es (J.R.R.-P.)

\* Correspondence: mgarclf@unileon.es



**Citation:** García-Fernández, M.; Sanz-Ablanedo, E.; Pereira-Obaya, D.; Rodríguez-Pérez, J.R. Vineyard Pruning Weight Prediction Using 3D Point Clouds Generated from UAV Imagery and Structure from Motion Photogrammetry. *Agronomy* **2021**, *11*, 2489. <https://doi.org/10.3390/agronomy11122489>

Academic Editors: Jitka Kumhálová, Jan Lukáš, Pavel Hamouz and Jose Antonio Dominguez-Gómez

Received: 16 November 2021

Accepted: 6 December 2021

Published: 8 December 2021

**Publisher's Note:** MDPI stays neutral with regard to jurisdictional claims in published maps and institutional affiliations.



**Copyright:** © 2021 by the authors. Licensee MDPI, Basel, Switzerland. This article is an open access article distributed under the terms and conditions of the Creative Commons Attribution (CC BY) license (<https://creativecommons.org/licenses/by/4.0/>).

**Abstract:** In viticulture, information about vine vigour is a key input for decision-making in connection with production targets. Pruning weight (PW), a quantitative variable used as indicator of vegetative vigour, is associated with the quantity and quality of the grapes. Interest has been growing in recent years around the use of unmanned aerial vehicles (UAVs) or drones fitted with remote sensing facilities for more efficient crop management and the production of higher quality wine. Current research has shown that grape production, leaf area index, biomass, and other viticulture variables can be estimated by UAV imagery analysis. Although SfM lowers costs, saves time, and reduces the amount and type of resources needed, a review of the literature revealed no studies on its use to determine vineyard pruning weight. The main objective of this study was to predict PW in vineyards from a 3D point cloud generated with RGB images captured by a standard drone and processed by SfM. In this work, vertical and oblique aerial images were taken in two vineyards of Godello and Mencía varieties during the 2019 and 2020 seasons using a conventional Phantom 4 Pro drone. Pruning weight was measured on sampling grids comprising 28 calibration cells for Godello and 59 total cells for Mencía (39 calibration cells and 20 independent validation). The volume of vegetation (V) was estimated from the generated 3D point cloud and PW was estimated by linear regression analysis taking V as predictor variable. When the results were leave-one-out cross-validated (LOOCV), the  $R^2$  was found to be 0.71 and the RMSE 224.5 (g) for the PW estimate in Mencía 2020, calculated for the 39 calibration cells on the grounds of oblique images. The regression analysis results for the 20 validation samples taken independently of the rest ( $R^2 = 0.62$ ; RMSE = 249.3 g) confirmed the viability of using the SfM as a fast, non-destructive, low-cost procedure for estimating pruning weight.

**Keywords:** drone; RGB imagery; structure from motion (SfM); viticulture; pruning weight

## 1. Introduction

The 107 million hectolitre international demand for wine in 2018 translated into EUR  $9 \times 10^9$  in export revenues for France, EUR  $6 \times 10^9$  for Italy, and EUR  $3 \times 10^9$  for Spain, although Spain exported a higher volume than either of its neighbours [1]. Those figures provide eloquent proof of the need to efficiently produce quality wine to compete effectively on an ever-more demanding market and ensure the profitability of wine production. That in turn calls for harvest monitoring and routine data gathering of vine parameters indicative of crop condition. Routine data collection of that nature enables farmers to adopt the sort of decisions early in the season that favour the production of higher quality wine at a lower cost.

Variables such as plant height, canopy volume or leaf area may afford growers with information on canopy structure, estimated production, and vine condition, parameters that can be used to predict harvest quantity and quality [2–5]. Such information was

traditionally acquired with conventional repetitive sampling-based methods that are normally slow, costly, and impractical where large areas are involved [6,7]. The vast resources required for such endeavours have induced researchers to analyse remote sensing tools to lower the economic cost of and time devoted to standard sampling for more efficient information gathering on vine condition [8].

Research exploring remote detection tools has led to the development of methods applying: laser image detection and ranging (LiDAR) to collect information on vine structure [7,9]; field spectroscopy to determine crop water content [10,11]; the MS Kinect device for pre-harvest production predictions [12]; and aerial photos from which to assess wine characteristics [13,14].

Imaging-based vineyard studies have focused particular attention on assessing the scans conducted with unmanned aerial vehicles (UAVs) or drones. Such interest has been sparked by the shorter time needed to plan flights and replace sensors, along with the lower cost and high geometric resolution and precision timing afforded by such platforms [15–18]. Thanks to UAV imagery biomass can be estimated, missing plants identified [19–21], vigour maps drawn [13,22], and quality variables predicted [23,24] from vegetation indices and digital image processing.

Advances in UAV-mediated technology and software have been applied by any number of researchers deploying structure from motion (SfM) photogrammetry to build high-precision three-dimensional models. SfM delivers point-cloud models at much lower expense than other technologies such as LiDAR. As SfM image orientation is based on automatic calibration, the procedure accommodates conventional non-metric cameras lacking calibration certificates, such as used in other studies to develop three-dimensional crop models [25]. Research deploying three-dimensional modelling has successfully gathered information on production quality variables such as harvest weight to estimate yield, leaf area index (LAI) for information on vineyard environmental conditions, and vine volume to improve crop management and reduce inputs [26–28].

Quality parameters include pruning weight (PW), a quantitative variable used as an indicator of plant vigour associated with the quantity and quality of the grapes harvested [29–31]. The smaller field sampling effort needed to collect information on this variable entails substantial cost savings for viticulturists redounding to more efficient production management.

A number of studies have been conducted to assess vine pruning weight with remote sensing methods [32–34]. Ground LiDAR-based techniques have contributed significantly to characterising and modelling vine structure from trunk and cordon volume and pruning weight [33]. As vine canopy volume can be used to estimate parameters related to pruning weight parameters such as biomass and leaf area, proximal imaging sensors are valid alternatives to traditional methods [32–34].

Multispectral aerial photographs have been used to map vineyard geometry-related vegetation indices such as NDVI (normalised difference vegetation index) and develop models for estimating pruning weight for which coefficients of determination upward of 0.75 have been reported [35,36]. UAV multispectral image-based pruning weight can be estimated by calculating relationships from infrared band-based vegetation indices (Pearson correlation coefficient,  $r = 0.58$ ) or regression models relating biomass to pruning debris determined with three-dimensional vineyard imaging [27,37]. In other UAV applications RGB imagery has been deployed to model vineyard geometry and estimate pruning weight with multiple linear regression taking geometric statistics such as the Pearson correlation, verified with root mean square error (RMSE), as predictor variables [38,39].

In light of the foregoing discussion, the main objective of this study was estimate pruning weight in vineyards from a 3D point cloud generated with conventional images captured by a standard drone and processed by structure from motion photogrammetry.

## 2. Materials and Methods

### 2.1. Study Area

The study area comprised two vineyards, each growing a different variety of grape, one Mencía and the other Godello. Both were located in Cacabelos, a municipality in the Spanish province of León. The 0.7 ha Mencía field (centre point coordinates: 683,675, 4,721,110 CRS UTM29N/ETRS89) was planted in 2005 with northeast to southwest-oriented trellises spaced at 1.8 m in rows and 1 m between rows. It stands at an altitude of 615 m on a 0–4.5% grade and features sandy-loam soil. Godello vineyard was planted in 2010 on a plot running from east to west and characterised by sandy loam soil. The field of Godello has 0.25 ha trellises characterised by 3.0 × 1.0 m spacing. Its centre point coordinates are 683,865, 4,720,475 CRS UTM29N/ETRS89 at an altitude of 595 m on land with a 0–2.3 % grade.

### 2.2. Experimental Procedure

The methodology applied is summarised in the flowchart in Figure 1. Field data collection consisted in selecting and geo-referencing the sampling plots and control points, UAV digital-imaging and pruning the vines and weighing the pruned wood. Digital image processing entailed building 3D point clouds for the vineyards, modelling the vine canopy and calculating sample cell volume. The cell volume-pruning weight curve was fitted using OLS linear regression, and the respective regression models were subsequently validated.

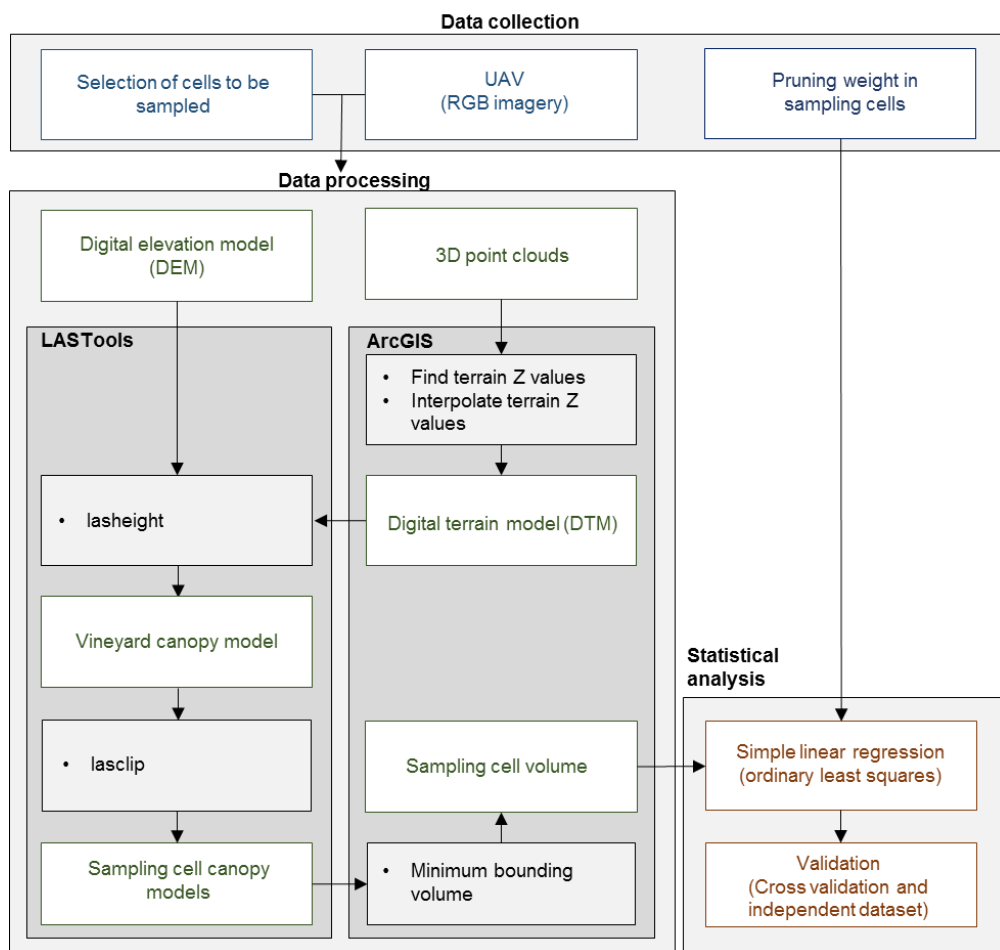


Figure 1. Methodology.

### 2.3. Sampling Cells

Two consecutive vines were selected as sampling cells. In the pattern followed for selection in the Mencía vineyard, the cells were spaced at a mean distance of 18.50 m in each row with five rows between one set of cells and the next. In the Godello field the cells were positioned on every other row and spaced at a mean in-row distance of 11.65 m. A total of 39 cells were selected to calibrate the Mencía data and 28 the Godello values. The cell arrangements in the two seasons studied are shown in Figure 2.



**Figure 2.** Sampling cell arrangement in the vineyards studied: (a), Mencía 2019; (b), Mencía 2020; (c), Godello 2019; (d), Godello 2020 (background images orthorectified for each vineyard and season).

In the 2020 season, 20 additional sample cells were selected in the Mencía vineyard for validation (black rectangles in Figure 2b).

The ground control points in all sampling cells were geo-referenced with a Leica Viva GNSS GS08 Plus receiver (Leica Geosystems A.G., Heerbrugg, Switzerland), working in RTK (real-time kinematics) mode and linked to the Castilla y León GNSS network (VRS3-format RTCM 3.0).

Pruning materials were weighed in situ at season end on a calibrated and fully levelled field scales.

#### 2.4. Drone Imaging

Drone images were captured on 1 August 2019 in the Mencía and 22 August in the Godello vineyard, whilst in 2020 the UAV was flown over both vineyards on the same date, 3 September. The images were captured beginning at 12:00 local time (UTC + 2 in daylight saving time) in optimal weather conditions, using a DJI Phantom 4 Professional UAV (SZ DJI Technology Co, Ltd., Shenzhen, China) fitted with a built-in DJI FC6310 sensor. Flights were programmed with DJI GS Pro (SZ DJI Technology Co, Ltd., Shenzhen, China) IOS software installed on an iPad. Transverse and longitudinal images were captured with 70 % overlaps and the exposure parameters such as aperture, exposure time, ISO sensitivity, and white balance were pre-set.

In 2019, the vineyards were scanned with vertical flight paths at altitudes of 40 m in Mencía and 30 m in Godello. In 2020, they were scanned obliquely, in Mencía at 20 m off the ground using a camera angle of  $-30^\circ$  and on Godello at a height of 24 m using a  $-60^\circ$  camera angle.

Nine ground control points each, uniformly distributed to geo-reference the images in the SRC UTM29N/ETRS 89 system were established at Mencía and Godello, measuring the coordinates with the GNSS receiver cited earlier. The flight parameters for each vineyard and season are summarised in Table 1.

**Table 1.** Flight parameters per vineyard and season.

Parameter	Mencía		Godello	
	2019	2020	2019	2020
Projection	Vertical	Oblique	Vertical	Oblique
Camera angle ( $^\circ$ )	$-90$	$-30$	$-90$	$-60$
Control points	9	9	9	9
Flight altitude (m)	40	20	30	24

#### 2.5. Digital Image Processing

The aerial images were processed using Agisoft Photoscan V1.3.1 (Agisoft LLC, St. Petersburg, Russia) commercial software, which uses structure from motion photogrammetry to reconstruct the surface by matching images and automatically identify homologous points in each orientation operation. The photogrammetric stages consisted of image alignment, sparse point model optimisation, dense point cloud construction, and orthoimage creation. Parameter values were calculated to the criteria recommended by the software developers. Images were aligned with the high accuracy feature enabled and the two preselection options provided (generic and reference); camera performance was optimised by calculating focal length ( $f$ ), principal point coordinates ( $c_x$ ,  $c_y$ ), radial distortion coefficients ( $k_1$ ,  $k_2$ ,  $k_3$ ), and tangential distortion coefficients ( $p_1$ ,  $p_2$ ); point clouds were processed with medium quality and no depth filtering, whilst orthoimages were built without colour correction. In this stage, control points were used to scale the model and correct camera parameter and reference coordinate misalignment errors. Dense point cloud construction was based on camera positions optimised by calculating unfiltered pairwise-aligned depth maps and applying the result to the final dense point cloud.

The 3D point cloud was processed to find the volume for each sampling cell using ArcGIS v10.7.1 (ESRI Inc., Redlands, CA, USA) GIS-based commercial software and LiDAR-based LAStools V1.4 (Rapidlasso GmbH, Gilching, Germany) software. A step-by-step approach was adopted to build (1) the digital terrain (DTM), (2) vineyard vegetation canopy model, (3) corresponding areas to sampling unit, and (4) sampling unit volume.

The DTM was developed using a dense point cloud DEM and ArcGIS v10.4.1 software. Both the DTM and the dense point cloud were exported in \*.las format and processed to build the vineyard vegetation canopy model, subsequently divided into sampling cells in shapefile format. The result was then processed using the ArcGIS v10.4.1 software

minimum bounding volume feature to calculate sampling cell volume, exported as tables. The features used at each step are given in Figure 1.

### 2.6. Pruning Weight Statistics

The primary pruning weight statistics are listed in Table 2, that include number of samples (No.), Minimum, Maximum, Range, Median, Mean, Standard Deviation (SD) and Coefficient of Variation (CV). As the pruning wood samples selected for weighing were drawn from the same field and season, the values were fairly uniform, with CV < 50 %, denoting reasonable scatter. The validation method used in this study was deemed suitable for the sample size and pruning weight variability observed.

**Table 2.** Pruning weight statistics.

Season	Vineyard	No.	Minimum (g)	Maximum (g)	Range (g)	Median (g)	Mean (g)	SD (g)	CV
2019	Mencía	39	200	2800	2600	1240	1307.18	527.49	40%
	Godello	28	400	3460	3060	1560	1792.14	754.63	42%
2020	Mencía	39	220	2220	2000	1000	1066.67	419.69	39%
	Godello	28	860	2680	1820	1410	1540.36	491.92	32%
	* Mencía	20	180	1840	1660	980	1026.50	370.98	36%

\* Mencía: separate dataset used for validation.

### 2.7. Statistical Analysis: Linear Regression and Validation

The linear regression equations relating predicted and observed data were formulated using ordinary least squares (OLS) methodology, taking vine volume (minimum bounding volume) as the predictor variable. The OLS methodology was previously evaluated by other researchers for the estimation of variables using aerial and satellite images [40,41]. Two methods were used to validate the results. Leave-one-out cross validation (LOOCV) was applied to validate the models built for each variety and season, running the procedure on R script further to the steps described in [42]. In that procedure one item is left out after each iteration and the rest of the sample used to fit the linear regression model. The prediction error was computed after each iteration and the process repeated for all possible combinations in the sample. The root mean square error (RMSE) and the coefficient of determination ( $R^2$ ) were taken to be the mean of all the respective values found for each LOOCV iteration. The second method involved separately validating the Mencía vineyard in 2020 using a dataset comprising 20 sample cells (Table 2).

## 3. Results

### 3.1. Digital Image Processing

The image orientation findings are summarised in Table 3. All the images captured by the drones were used to build the point cloud. Of the 426 images collected for the Mencía variety in 2020, the points could be positioned for only 352, whereas all the images comprising the other three cases could be used in the model.

The orthoimages obtained for the Mencía variety in the 2019 season (Figure 2a) featured 1 cm, and those for the 2020 season 0.5 cm, pixel spatial resolution (Figure 2b). The orthoimages for the Godello variety in the 2019 season exhibited 0.8 cm (Figure 2c) and those for the 2020 season 0.6 cm (Figure 2d) pixel spatial resolution. The orthoimages were obtained with the setup summarised in Table 1.

The root mean square errors of the control points ( $RMSE_{XYZ}$ ) ranged from 5.0 to 9.0 cm in the Mencía vineyard and from 3.7 to 7.0 cm in the Godello vineyard. These positioning error values of the control points were deemed to be reasonable and acceptable for the present research [43,44]. In both vineyards, the smallest  $RMSE_{XYZ}$  were found for the images an oblique angle, which were taken in 2020 season ( $RMSE_{XYZ} = 5.0$  cm in Mencía and  $RMSE_{XYZ} = 3.7$  cm in Godello).

**Table 3.** Digital processing data calculated with structure from motion procedures for UAV images captured in the Mencía and Godello vineyards in 2019 and 2020.

Parameter	Mencía		Godello	
	2019	2020	2019	2020
No. of cameras	172	426	141	385
No. of aligned cameras	172	352	141	385
RMSE <sub>XYZ</sub> (cm)	9.0	5.0	7.0	3.7
GSD (cm/pix)	1.0	0.5	0.8	0.6
Dense point cloud				
Total No. of points	22,468,598	56,160,935	16,538,552	33,755,521
No. of sample cell points	93,108	210,653	153,028	281,214

Point cloud densification for the Mencía variety generated a total of nearly 22.5 M points in the 2019 season and 56 M in 2020, with 93,108 attributable to sampling cells in 2019 and 210,653 in 2020. Analogously, point cloud densification for the Godello variety generated a total of round 16.5 M points in 2019 season and just under 34 M in 2020, with 153,028 attributable to sampling cells in 2019 and 281,214 in 2020.

### 3.2. Statistical Analysis of Prediction Model Results

Predicted PW is plotted against observed pruning weight for the four cases studied in Figure 3 (Mencía 2019 in Figure 3a, Godello 2019 in Figure 3b, Mencía 2020 in Figure 3c, and Godello 2020 in Figure 3d), for which regression analysis identified good fits using calculated volume (V) like predictor variable.

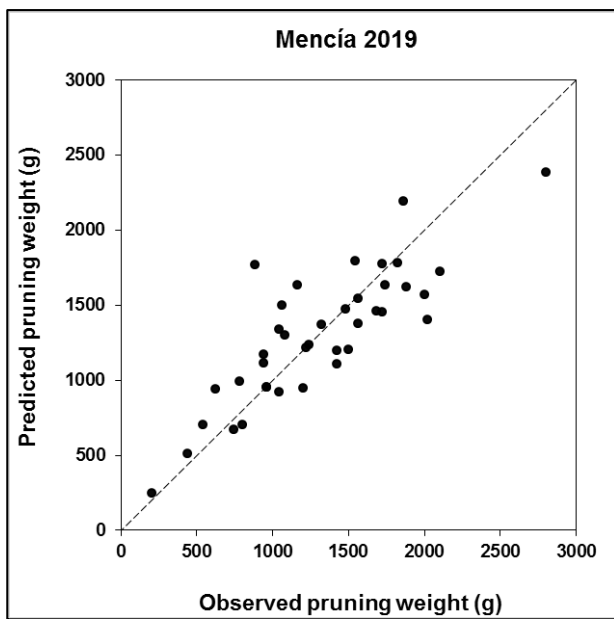
Table 4 shows the result of the goodness of fit calculated by LOOCV of the linear regression models of the Figure 3, where LOOCV validation model were for Mencía 2019  $R^2 = 0.66$  and  $RMSE = 304.5$  g; for Godello 2019  $R^2 = 0.68$  and  $RMSE = 421.1$  g; for Mencía 2020  $R^2 = 0.71$  and  $RMSE = 224.5$  g; and for Godello 2020  $R^2 = 0.56$  and  $RMSE = 319.9$  g.

**Table 4.** Results of leave-one-out cross validation for predicted pruning weight.

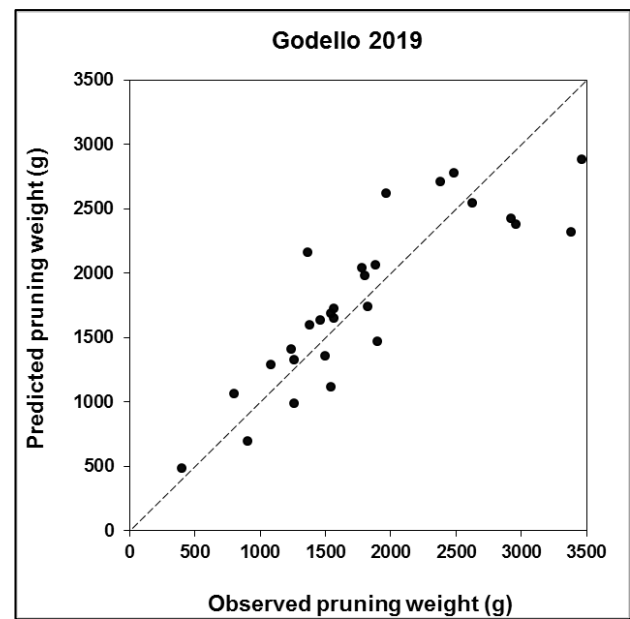
Data Set	Equation	$R^2$	RMSE (g)
Mencía 2019	$PW = 2279.7 V - 560.1$	0.66	304.5
Godello 2019	$PW = 2293.0 V - 531.5$	0.68	421.1
Mencía 2020	$PW = 1572.6 V + 37.4$	0.71	224.5
Godello 2020	$PW = 1862.1 V + 149.3$	0.56	319.9

PW: pruning weight; V: volume.

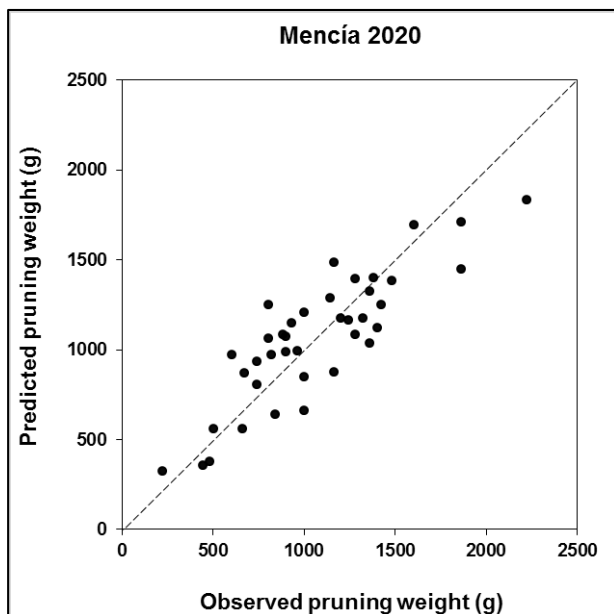
Figure 4 plots predicted PW against observed pruning weight for the Mencía validation calculated using the photogrammetric procedure described in Section 2.5. A fairly close correlation was found with the respective regression analysis, with  $R^2 = 0.62$  and  $RMSE = 249.3$  g.



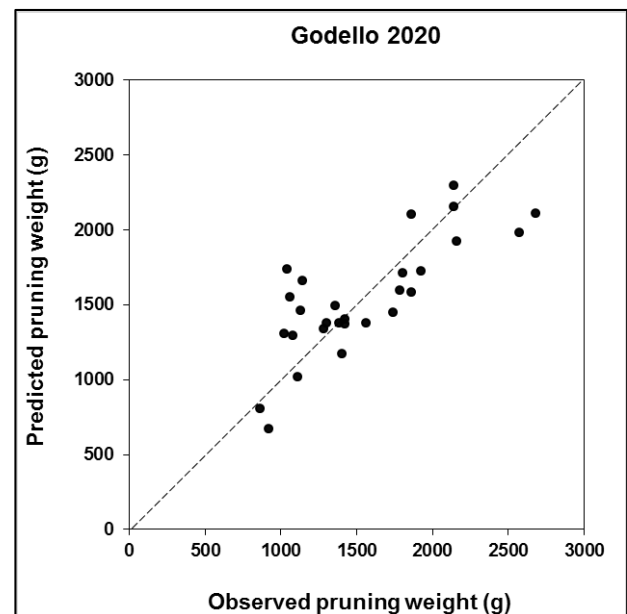
(a)



(b)



(c)



(d)

**Figure 3.** Predicted vs. observed pruning weight validated with the leave-one-out cross procedure for: (a) Mencía 2019; (b) Godello 2019; (c) Mencía 2020; (d) Godello 2020 (dashed lines = 1:1).



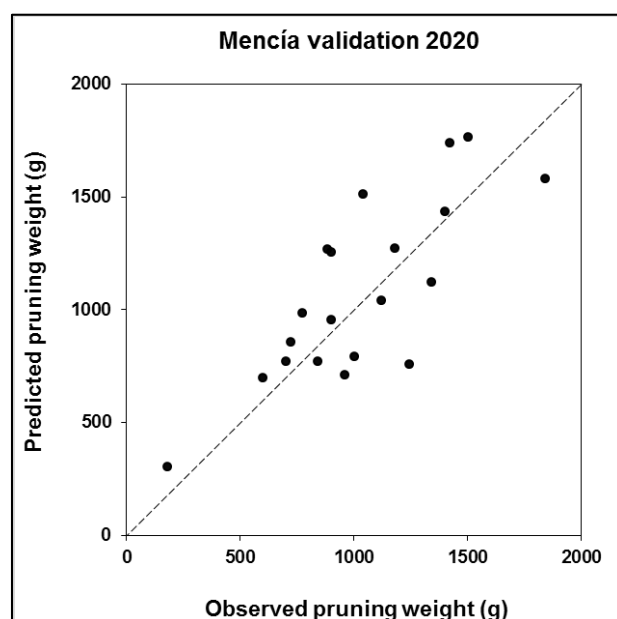


**Figure 4.** Predicted vs. observed pruning weight for the Mencía vineyard validated with independently collected data (dashed line = 1.1).

#### 4. Discussion

This study aimed primarily to assess RGB images captured by a low-cost drone to predict pruning weight in two varieties of grapevines from point clouds generated with structure-of-motion photogrammetry. Point clouds for precision viticulture studies are typically built from data acquired by LiDAR sensors in aerial or ground platforms to model canopy structure and calculate quantitative grapevine biomass variables. The use of such sensors may prove too costly to ensure crop profitability at a given end product market value. Drone-mediated conventional imaging is both a viable alternative, delivering results apt for accurate vine modelling and generally more affordable in terms of cost and resources.

Here point clouds were built from SfM-processed images [45]. As the sensor used was geometrically calibrated via photogrammetry, the control points defined yielded a high-precision three-dimensional model of the geo-referenced crop [46]. The relationship between pruning weight and the respective point clouds was calculated in the laboratory using linear regression.

UAV images were captured both vertically and obliquely for use in pruning weight predictions. The validation data for the 2019 season when the UAV captured the images at a 90° angle were, for Mencía 2019  $R^2 = 0.66$  and RMSE = 304.5 g; and for Godello 2019  $R^2 = 0.68$  and RMSE 421.1 g. The results for the oblique scanning conducted in the 2020 season were, for Mencía 2020  $R^2 = 0.71$  and RMSE 224.5 g; and for Godello 2020  $R^2 = 0.56$  and RMSE = 319.9 g (Table 4). Attention is drawn to the particularly high accuracy for Mencía 2020.

In earlier studies estimating quantitative variables such as crop height or leaf area index the authors found that that precision could be enhanced by including oblique images in the data analysed [47–49]. Those reports are consistent with the data given in Table 3, according to which the positioning error for the reconstructed control points (RMSE<sub>XYZ</sub>) was smaller where oblique imaging was deployed [48].

Oblique photogrammetry delivered a 2.26-fold larger number of sampling cell data points than vertical photogrammetry for the Mencía vineyard and 1.83-fold more for the Godello vineyard (Table 3). The  $R^2$  for the cell canopy volume calculated to estimate pruning weight was higher in the model generated from oblique photographs (Figure 5). That finding was consistent with the data recorded by Che et al. [47], who found oblique

images to improve the correlation in the SfM-generated three-dimensional model used to estimate vegetation canopy parameters.

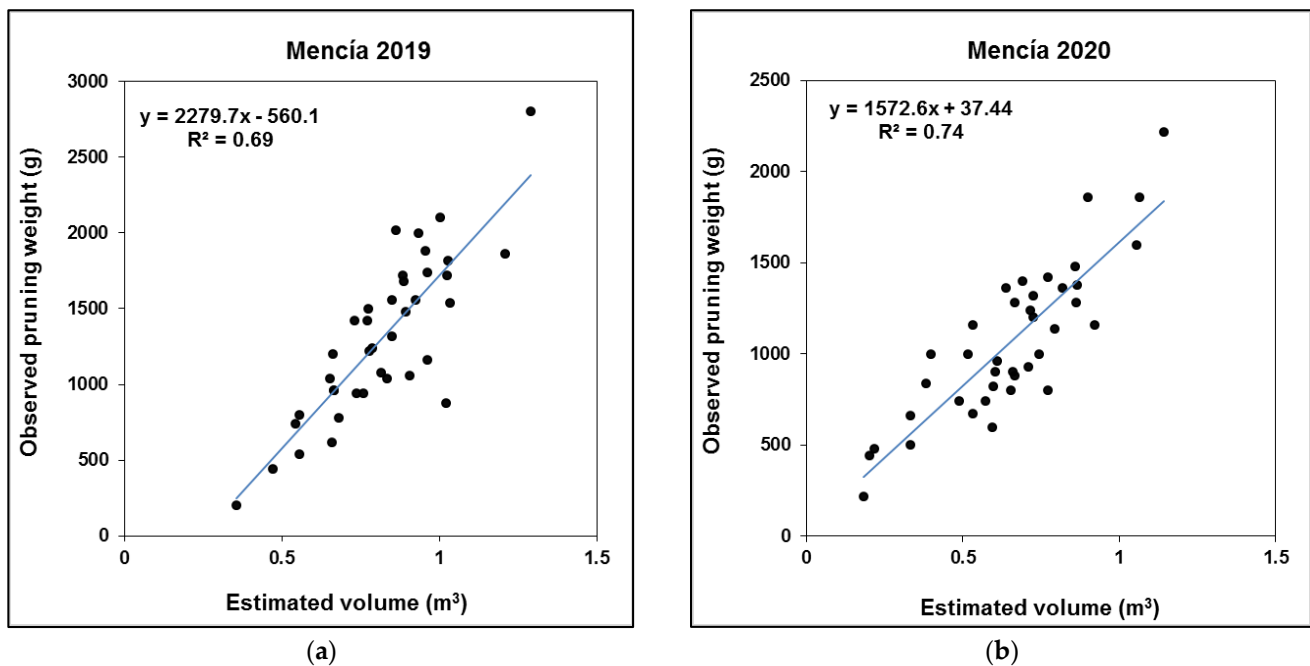


**Figure 5.** Observed pruning weight vs. estimated volume and respective regression lines for: (a) Mencía 2019; and (b) Mencía 2020 (solid line = linear regression).

The findings for the Godello vineyard in 2020 are not consistent with the results reported for earlier studies or those found here for the Mencía vineyard. The green pruning conducted at Godello during the 2020 vegetative cycle affected the weight of the debris.

Our results demonstrate volume of vine canopy was a variable that allows estimating pruning weight from drone images and SfM photogrammetry. The resulting 3D point cloud was processed with LAsTool LiDAR point cloud software and the ArGIS graphic information system. That methodology yields a geometric figure adjusted to the irregular shape of the vine structures that enhances the quantitative estimates of parameter values, in which the presence of voids in the vegetation is also taken into consideration [20]. The  $R^2 = 0.74$  coefficient of determination found in this study for the relationship between pruning weight and the volume so calculated supports the viability of using SfM to determine vine quantitative variables, a finding in line with earlier reports [20,50,51].

The present research confirmed the feasibility of estimating pruning weight from photogrammetrically processed drone images. Based on 3D point-cloud processing, the pruning weight predicted with this approach was validated with independently collected data (Table 4, Mencía 2020). The scientific literature corroborates the validity of using point clouds to predict pruning weight from data collected by ground vehicles fitted with sensors [32,52,53].

Tagarakis et al. [52] and Siebers et al. [32] showed that ground LiDAR could be used to estimate that parameter. The Tagarakis et al. [52] findings for the relationship between the LiDAR data and vine parameters based on scanning impact maps were closely correlated (Pearson correlation coefficient,  $r = 0.83$ ;  $p < 0.01$ ). An even higher coefficient was obtained with the methodology proposed by Siebers et al. [32], in which the volume found with the LiDAR point cloud was used to predict pruning weight. Their method was tested in the present study in which the cloud was built with points obtained by UAV-captured RGB images.

LiDAR is an investment-intensive method, however, whereas low-cost sensors would be more affordable for farmers. Further to that reasoning, Moreno et al. [53] deployed

a low-sweep sensor to estimate pruning weight. They nonetheless concluded that their method might not be wholly suitable for narrow canopy areas with low and scantily robust correlations and that the results of simple linear regression validation might be impacted by the number of fields analysed. The advantage of using the leave-one-out cross validation approach adopted in our study enhanced the reliability of the results compared to the method used in Moreno et al. [53].

## 5. Conclusions

A photogrammetric method using RGB imagery was applied to predict vineyard pruning weight. Using a dense point cloud (DPC) generated with a structure from motion (SfM) algorithm, vine volume was calculated by modelling the minimum bounding volume. Linear regression was then used to estimate pruning weight from vine volume as the predictor variable. Model accuracy was assessed with cross validation (two years' data) and a separate dataset (for one year). The  $R^2$  found with cross validation ranged from 0.66 to 0.71 for the Mencía vineyard and 0.56 to 0.68 for the Godello field. Although precision and accuracy predictions were variety- and season-dependent, the quality of the respective estimates suffices to use information on pruning weight or related parameters as proxies for vine vigour. The present findings attest to the usability of UAVs as speedy, cost-effective, and non-destructive platforms for estimating vineyard pruning weight. Future precision viticulture research will focus on the application of UAV imagery to characterise vineyard structure.

**Author Contributions:** Conceptualisation: M.G.-F., D.P.-O., E.S.-A. and J.R.R.-P.; methodology: M.G.-F., E.S.-A. and J.R.R.-P.; software: D.P.-O. and E.S.-A.; formal analysis: M.G.-F. and E.S.-A.; writing—original draft preparation: M.G.-F., D.P.-O., E.S.-A. and J.R.R.-P.; writing—review and editing: M.G.-F., E.S.-A. and J.R.R.-P.; visualisation: D.P.-O., E.S.-A. and J.R.R.-P.; supervision and project administration: J.R.R.-P. All authors have read and agreed to the published version of the manuscript.

**Funding:** This research was funded by the Education Department of the Junta de Castilla y León, grant number LE112G18.

**Institutional Review Board Statement:** Not applicable.

**Informed Consent Statement:** Not applicable.

**Data Availability Statement:** Data sharing not applicable.

**Acknowledgments:** This study was funded by the Regional Government of Castilla y León's Department of Education under grant LE112G18, awarded in a tender called for qualified research groups affiliated with public universities, conditional upon a 2018 starting date (Order of 20 November 2017). Marta García Fernández gratefully acknowledges financial support provided by Fundación Carolina Rodríguez and Universidad de León.

**Conflicts of Interest:** The authors declare no conflict of interest. The authors declare that they have no known competing financial interests or personal relationships that could have appeared to influence the work reported in this paper.

## References

1. OIV. *OIV–International Organization of Vine and Wine; Statistics*; OIV: Paris, France, 2019.
2. Malambo, L.; Popescu, S.C.; Murray, S.C.; Putman, E.; Pugh, N.A.; Horne, D.W.; Richardson, G.; Sheridan, R.; Rooney, W.L.; Avant, R.; et al. Multitemporal Field-Based Plant Height Estimation Using 3D Point Clouds Generated from Small Unmanned Aerial Systems High-Resolution Imagery. *Int. J. Appl. Earth Obs. Geoinf.* **2018**, *64*, 31–42. [[CrossRef](#)]
3. Andújar, D.; Moreno, H.; Bengochea-Guevara, J.M.; de Castro, A.; Ribeiro, A. Aerial Imagery or On-Ground Detection? An Economic Analysis for Vineyard Crops. *Comput. Electron. Agric.* **2019**, *157*, 351–358. [[CrossRef](#)]
4. Ouyang, J.; Bei, R.D.; Fuentes, S.; Collins, C. UAV and Ground-Based Imagery Analysis Detects Canopy Structure Changes after Canopy Management Applications. *OENO One* **2020**, *54*, 1093–1103. [[CrossRef](#)]
5. White, W.A.; Alsina, M.M.; Nieto, H.; McKee, L.G.; Gao, F.; Kustas, W.P. Determining a Robust Indirect Measurement of Leaf Area Index in California Vineyards for Validating Remote Sensing-Based Retrievals. *Irrig. Sci.* **2019**, *37*, 269–280. [[CrossRef](#)]

6. Rosell Polo, J.R.; Sanz Cortiella, R.; Llorens Calveras, J.; Arnó Satorra, J.; Escolà i Agustí, A.; Ribes Dasi, M.; Masip Vilalta, J.; Camp, F.; Gràcia, F.; Solanelles Batlle, F.; et al. A Tractor-Mounted Scanning LIDAR for the Non-Destructive Measurement of Vegetative Volume and Surface Area of Tree-Row Plantations: A Comparison with Conventional Destructive Measurements. *Biosyst. Eng.* **2009**, *102*, 128–134. [[CrossRef](#)]
7. Mashalaba, L.; Galleguillos, M.; Seguel, O.; Poblete-Olivares, J. Predicting Spatial Variability of Selected Soil Properties Using Digital Soil Mapping in a Rainfed Vineyard of Central Chile. *Geoderma Reg.* **2020**, *22*, e00289. [[CrossRef](#)]
8. Arnó, J.; Escolà, A.; Rosell-Polo, J.R. Setting the Optimal Length to Be Scanned in Rows of Vines by Using Mobile Terrestrial Laser Scanners. *Precis. Agric.* **2017**, *18*, 145–151. [[CrossRef](#)]
9. Cheraïet, A.; Naud, O.; Carra, M.; Codis, S.; Lebeau, F.; Taylor, J. An Algorithm to Automate the Filtering and Classifying of 2D LiDAR Data for Site-Specific Estimations of Canopy Height and Width in Vineyards. *Biosyst. Eng.* **2020**, *200*, 450–465. [[CrossRef](#)]
10. González-Fernández, A.B.; Sanz-Ablanedo, E.; Gabella, V.M.; García-Fernández, M.; Rodríguez-Pérez, J.R. Field Spectroscopy: A Non-Destructive Technique for Estimating Water Status in Vineyards. *Agronomy* **2019**, *9*, 427. [[CrossRef](#)]
11. Barnard, Y.; Strever, A.; Bosman, G.; Poblete-Echeverría, C. Fast and Non-Destructive Method for Estimating Grapevine Water Status. *Acta Hort.* **2019**, *1253*, 413–420. [[CrossRef](#)]
12. Marinello, F.; Pezzuolo, A.; Cillis, D.; Sartori, L. Kinect 3D Reconstruction for Quantification of Grape Bunches Volume and Mass. *Eng. Rural. Dev.* **2016**, *15*, 876–881.
13. Campos, J.; García-Ruíz, F.; Gil, E. Assessment of Vineyard Canopy Characteristics from Vigour Maps Obtained Using Uav and Satellite Imagery. *Sensors* **2021**, *21*, 2363. [[CrossRef](#)]
14. Vélez, S.; Rubio, J.A.; Andrés, M.I.; Barajas, E. Agronomic Classification between Vineyards ('Verdejo') Using NDVI and Sentinel-2 and Evaluation of Their Wines. *Vitis J. Grapevine Res.* **2019**, *58*, 33–38. [[CrossRef](#)]
15. Matese, A.; Di Gennaro, S.F.; Santesteban, L.G. Methods to Compare the Spatial Variability of UAV-Based Spectral and Geometric Information with Ground Autocorrelated Data. A Case of Study for Precision Viticulture. *Comput. Electron. Agric.* **2019**, *162*, 931–940. [[CrossRef](#)]
16. Matese, A.; Toscano, P.; Di Gennaro, S.F.; Genesio, L.; Vaccari, F.P.; Primicerio, J.; Belli, C.; Zaldei, A.; Bianconi, R.; Gioli, B. Intercomparison of UAV, Aircraft and Satellite Remote Sensing Platforms for Precision Viticulture. *Remote Sens.* **2015**, *7*, 2971–2990. [[CrossRef](#)]
17. Hassler, S.C.; Baysal-Gurel, F. Unmanned Aircraft System (UAS) Technology and Applications in Agriculture. *Agronomy* **2019**, *9*, 618. [[CrossRef](#)]
18. Ronchetti, G.; Pagliari, D.; Sona, G. DTM Generation through UAV Survey with a Fisheye Camera on a Vineyard. *Int. Arch. Photogramm. Remote Sens. Spatial Inf. Sci.* **2018**, *XLII-2*, 983–989. [[CrossRef](#)]
19. Matese, A.; Cinat, P.; Romboli, Y.; Berton, A.; Di Gennaro, S.F. Missing plant detection and biomass estimation from 3D models generated from UAV in a vineyard. In *Precision Agriculture '19*; Wageningen Academic Publishers: Wageningen, The Netherlands, 2019; pp. 165–172. [[CrossRef](#)]
20. Di Gennaro, S.F.; Matese, A. Evaluation of Novel Precision Viticulture Tool for Canopy Biomass Estimation and Missing Plant Detection Based on 2.5D and 3D Approaches Using RGB Images Acquired by UAV Platform. *Plant Methods* **2020**, *16*, 91. [[CrossRef](#)] [[PubMed](#)]
21. Bendig, J.; Yu, K.; Aasen, H.; Bolten, A.; Bennertz, S.; Broscheit, J.; Gnyp, M.L.; Bareth, G. Combining UAV-Based Plant Height from Crop Surface Models, Visible, and near Infrared Vegetation Indices for Biomass Monitoring in Barley. *Int. J. Appl. Earth Obs. Geoinf.* **2015**, *39*, 79–87. [[CrossRef](#)]
22. Duarte, L.; Teodoro, A.C.; Sousa, J.J.; Pádua, L. QVigourMap: A GIS Open Source Application for the Creation of Canopy Vigour Maps. *Agronomy* **2021**, *11*, 952. [[CrossRef](#)]
23. García-Fernández, M.; Sanz-Ablanedo, E.; Rodríguez-Pérez, J.R. High-Resolution Drone-Acquired RGB Imagery to Estimate Spatial Grape Quality Variability. *Agronomy* **2021**, *11*, 655. [[CrossRef](#)]
24. Bonilla, I.; Toda, F.M.d.; Martínez-Casasnovas, J.A. Vine Vigor, Yield and Grape Quality Assessment by Airborne Remote Sensing over Three Years: Analysis of Unexpected Relationships in Cv. Tempranillo. *Span. J. Agric. Res.* **2015**, *13*, 0903. [[CrossRef](#)]
25. Tucci, G.; Parisi, E.I.; Castelli, G.; Errico, A.; Corongiu, M.; Sona, G.; Viviani, E.; Bresci, E.; Preti, F. Multi-Sensor UAV Application for Thermal Analysis on a Dry-Stone Terraced Vineyard in Rural Tuscany Landscape. *ISPRS Int. J. Geo-Inf.* **2019**, *8*, 87. [[CrossRef](#)]
26. Torres-Sánchez, J.; Mesas-Carrascosa, F.J.; Santesteban, L.-G.; Jiménez-Brenes, F.M.; Oñeca, O.; Villa-Llop, A.; Loidi, M.; López-Granados, F. Grape Cluster Detection Using UAV Photogrammetric Point Clouds as a Low-Cost Tool for Yield Forecasting in Vineyards. *Sensors* **2021**, *21*, 3083. [[CrossRef](#)]
27. Comba, L.; Biglia, A.; Ricauda Aimonino, D.; Tortia, C.; Mania, E.; Guidoni, S.; Gay, P. Leaf Area Index Evaluation in Vineyards Using 3D Point Clouds from UAV Imagery. *Precis. Agric.* **2020**, *21*, 881–896. [[CrossRef](#)]
28. De Castro, A.I.; Jiménez-Brenes, F.M.; Torres-Sánchez, J.; Peña, J.M.; Borra-Serrano, I.; López-Granados, F. 3-D Characterization of Vineyards Using a Novel UAV Imagery-Based OBIA Procedure for Precision Viticulture Applications. *Remote Sens.* **2018**, *10*, 584. [[CrossRef](#)]
29. Weaver, R.J. *Grape Growing*, 1st ed.; John Wiley & Sons: Hoboken, NJ, USA, 1976.
30. Keller, M. *The Science of Grapevines*, 3rd ed.; Elsevier: Amsterdam, The Netherlands, 2020.
31. Senthilkumar, S.; Vijayakumar, R.M.; Soorianathasundaram, K.; Devi, D.D. Effect of Pruning Severity on Vegetative, Physiological, Yield and Quality Attributes in Grape (*Vitis Vinifera* L.)—A Review. *Curr. Agric. Res.* **2015**, *3*, 42–54. [[CrossRef](#)]

32. Siebers, M.H.; Edwards, E.J.; Jimenez-Berni, J.A.; Thomas, M.R.; Salim, M.; Walker, R.R. Fast Phenomics in Vineyards: Development of GROver, the Grapevine Rover, and LiDAR for Assessing Grapevine Traits in the Field. *Sensors* **2018**, *18*, 2924. [[CrossRef](#)] [[PubMed](#)]
33. Moreno, H.; Valero, C.; Bengochea-Guevara, J.M.; Ribeiro, Á.; Garrido-Izard, M.; Andújar, D. On-Ground Vineyard Reconstruction Using a LiDAR-Based Automated System. *Sensors* **2020**, *20*, 1102. [[CrossRef](#)] [[PubMed](#)]
34. Sanz, R.; Llorens, J.; Escolà, A.; Arnó, J.; Planas, S.; Román, C.; Rosell-Polo, J.R. LIDAR and Non-LIDAR-Based Canopy Parameters to Estimate the Leaf Area in Fruit Trees and Vineyard. *Agric. For. Meteorol.* **2018**, *260–261*, 229–239. [[CrossRef](#)]
35. Towers, P.; Strever, A.; Poblete-Echeverría, C. Estimation of Vine Pruning Weight Using Remote Sensing Data: Relative Contribution of Variables. In Proceedings of the Encuentro Internacional Vitivinícola XX GiESCO 2017, Mendoza, Argentina, 5–9 November 2017.
36. Dobrowski, S.Z.; Ustin, S.L.; Wolpert, J.A. Grapevine Dormant Pruning Weight Prediction Using Remotely Sensed Data. *Aust. J. Grape Wine Res.* **2003**, *9*, 177–182. [[CrossRef](#)]
37. Rey-Caramés, C.; Diago, M.P.; Martín, M.P.; Lobo, A.; Tardaguila, J. Using RPAS Multi-Spectral Imagery to Characterise Vigour, Leaf Development, Yield Components and Berry Composition Variability within a Vineyard. *Remote Sens.* **2015**, *7*, 14458–14481. [[CrossRef](#)]
38. Pádua, L.; Marques, P.; Hruška, J.; Adão, T.; Peres, E.; Morais, R.; Sousa, J.J. Multi-Temporal Vineyard Monitoring through UAV-Based RGB Imagery. *Remote Sens.* **2018**, *10*, 1907. [[CrossRef](#)]
39. Ghiani, L.; Sassu, A.; Lozano, V.; Brundu, G.; Piccirilli, D.; Gambella, F. Use of UAVs and Canopy Height Model Applied on a Time Scale in the Vineyard. In *Innovative Biosystems Engineering for Sustainable Agriculture, Forestry and Food Production*; Coppola, A., Di Renzo, G.C., Altieri, G., D’Antonio, P., Eds.; Springer International Publishing: Cham, Germany, 2020; pp. 837–844.
40. Rocha Neto, O.C.d.; Teixeira, A.D.S.; Leão, R.A.d.O.; Moreira, L.C.J.; Galvão, L.S. Hyperspectral Remote Sensing for Detecting Soil Salinization Using ProSpecTIR-VS Aerial Imagery and Sensor Simulation. *Remote Sens.* **2017**, *9*, 42. [[CrossRef](#)]
41. Escoto, J.E.; Blanco, A.C.; Argamosa, R.J.; Medina, J.M. Pasig River Water Quality Estimation Using An Empirical Ordinary Least Squares Regression Model Of Sentinel-2 Satellite Images. *Int. Arch. Photogramm. Remote Sens. Spatial Inf. Sci.* **2021**, *XLVI-4/W6-2021*, 161–168. [[CrossRef](#)]
42. Hastie, T.; Tibshirani, R.; Friedman, J.H. *The Elements of Statistical Learning: Data Mining, Inference, and Prediction*, 2nd ed.; Springer Series in Statistics; Springer: New York, NY, USA, 2009; ISBN 978-0-387-84857-0.
43. Sanz-Ablanedo, E.; Chandler, J.H.; Rodríguez-Pérez, J.R.; Ordóñez, C. Accuracy of Unmanned Aerial Vehicle (UAV) and SfM Photogrammetry Survey as a Function of the Number and Location of Ground Control Points Used. *Remote Sens.* **2018**, *10*, 1606. [[CrossRef](#)]
44. Martínez-Carricondo, P.; Agüera-Vega, F.; Carvajal-Ramírez, F.; Mesas-Carrascosa, F.-J.; García-Ferrer, A.; Pérez-Porras, F.-J. Assessment of UAV-Photogrammetric Mapping Accuracy Based on Variation of Ground Control Points. *Int. J. Appl. Earth Obs. Geoinf.* **2018**, *72*, 1–10. [[CrossRef](#)]
45. Westoby, M.J.; Brasington, J.; Glasser, N.F.; Hambrey, M.J.; Reynolds, J.M. ‘Structure-from-Motion’ Photogrammetry: A Low-Cost, Effective Tool for Geoscience Applications. *Geomorphology* **2012**, *179*, 300–314. [[CrossRef](#)]
46. Garcia, M.V.Y.; Oliveira, H.C. The Influence Of Ground Control Points Configuration And Camera Calibration For Dtm And Orthomosaic Generation Using Imagery Obtained From A Low-Cost UAV. *ISPRS Ann. Photogramm. Remote Sens. Spatial Inf. Sci.* **2020**, *V-1-2020*, 239–244. [[CrossRef](#)]
47. Che, Y.; Wang, Q.; Xie, Z.; Zhou, L.; Li, S.; Hui, F.; Wang, X.; Li, B.; Ma, Y. Estimation of Maize Plant Height and Leaf Area Index Dynamics Using an Unmanned Aerial Vehicle with Oblique and Nadir Photography. *Ann. Bot.* **2020**, *126*, 765–773. [[CrossRef](#)] [[PubMed](#)]
48. Lin, L.; Yu, K.; Yao, X.; Deng, Y.; Hao, Z.; Chen, Y.; Wu, N.; Liu, J. UAV Based Estimation of Forest Leaf Area Index (LAI) through Oblique Photogrammetry. *Remote Sens.* **2021**, *13*, 803. [[CrossRef](#)]
49. Zhou, X.; Zhang, X. Individual Tree Parameters Estimation for Plantation Forests Based on UAV Oblique Photography. *IEEE Access* **2020**, *8*, 96184–96198. [[CrossRef](#)]
50. López-Granados, F.; Torres-Sánchez, J.; Jiménez-Brenes, F.M.; Oneka, O.; Marín, D.; Loidi, M.; de Castro, A.I.; Santesteban, L.G. Monitoring Vineyard Canopy Management Operations Using UAV-Acquired Photogrammetric Point Clouds. *Remote Sens.* **2020**, *12*, 2331. [[CrossRef](#)]
51. Comba, L.; Biglia, A.; Ricauda Aimonino, D.; Gay, P. Unsupervised Detection of Vineyards by 3D Point-Cloud UAV Photogrammetry for Precision Agriculture. *Comput. Electron. Agric.* **2018**, *155*, 84–95. [[CrossRef](#)]
52. Tagarakis, A.C.; Koundouras, S.; Fountas, S.; Gemtos, T. Evaluation of the Use of LIDAR Laser Scanner to Map Pruning Wood in Vineyards and Its Potential for Management Zones Delineation. *Precis. Agric.* **2018**, *19*, 334–347. [[CrossRef](#)]
53. Moreno, H.; Rueda-Ayala, V.; Ribeiro, A.; Bengochea-Guevara, J.; Lopez, J.; Peteinatos, G.; Valero, C.; Andújar, D. Evaluation of Vineyard Cropping Systems Using On-Board RGB-Depth Perception. *Sensors* **2020**, *20*, 6912. [[CrossRef](#)]